

## Adsorption of Selected Heavy Metals Using Agricultural Waste: Equilibrium, Kinetic and Thermodynamic Studies

Nnaemeka J. Okorochoa<sup>1</sup>, Enyinnaya P. Nwojo<sup>2</sup>, Ikechukwu O. Achinihu<sup>3</sup>,  
Maureen O. Chijioke-Okere<sup>4</sup>, Basil N. Anukam<sup>5</sup>, Chijioke E. Omaliko<sup>6</sup>

<sup>1,6</sup> (Department of pure and industrial chemistry, College of physical sciences/ University of Calabar, Nigeria)

<sup>2</sup> (Department of pure and industrial chemistry, College of science/ University of Port Harcourt, Nigeria)

<sup>3</sup> (Department of chemistry, College of sciences/ Alvan Ikoku Federal College of Education Owerri, Nigeria)

<sup>4,5</sup> (Department of chemistry, College of physical sciences/ Federal University of Technology Owerri, Nigeria)

Corresponding Author: (N. J. Okorochoa)

**ABSTRACT:** The use of raw maize cob (rmc) as a natural adsorbent for the removal of  $Pb^{2+}$  and  $Cu^{2+}$  ions from simulated waste water was studied. Batch experiments were carried out to verify the influence of varying contact time, initial metal ion concentration, adsorbent dosage, pH and temperature of adsorption. Adsorption increases with increasing adsorbent dosage for the two metal ions. It also increases with increase in temperature from 20 °C to 70 °C for  $Cu^{2+}$  but decreases with temperature increase for  $Pb^{2+}$  in the same temperature range. The maximum adsorption of  $Pb^{2+}$  was found to be 92.68 % at contact time of 105 minutes and pH of 6. The adsorption of  $Cu^{2+}$  was found to be maximum 89.15 % at pH of 12 and contact time of 75 minutes. Thermodynamic analysis suggested that the adsorption of  $Pb^{2+}$  was spontaneous and exothermic in nature (negative  $\Delta G$ ,  $\Delta S$  and  $\Delta H$  parameters), while that of  $Cu^{2+}$  was also spontaneous but endothermic in nature (negative  $\Delta G$  and positive  $\Delta H$  &  $\Delta S$  parameter). The kinetics of the adsorption of  $Cu^{2+}$  and  $Pb^{2+}$  on the adsorbent (rmc) was evaluated using five different models thus the Pseudo-second order kinetic model provided an appropriate depiction of the metal ions adsorption. Six (6) different adsorption isotherm models were examined and correlated, thus the fitted models for this adsorption reaction were in the order of Langmuir > Freundlich > Temkin > Halsey isotherm models. FTIR and SEM analysis were carried out on rmc and it showed that raw maize cob has active pores and ionizable functional groups at the surface.

**Keywords:** Adsorption, Copper, Isotherms, Kinetics, Lead, Raw maize cob.

Date of Submission: 27-11-2019

Date of Acceptance: 12-12-2019

### I. INTRODUCTION

Adequate supply of fresh and clean water is a basic need for all human beings on the earth, but millions of people from destitute sections of the society are deprived of fresh and clean water and are forced to take contaminated water. Fresh water sources all over the world are threatened due to poor management, ecological degradation and over exploitation [1]. Heavy metals like Cr, Ni, Cd, Pb, Cu, Zn etc are not biodegradable, unlike organic pollutants which are biodegradable and their increasing concentration in the environment is detrimental to a variety of living species. They are mainly released through anthropogenic means in the environment of which, some are the major pollutants of soil and water resources [2].

Some metals such as Copper, Zinc and iron are considered bio-essential to humans while others such as Cadmium, Lead, Mercury and chromium are highly toxic even at low concentrations. However, even bio-essential metals may cause physiological and ecological problems if present at certain higher concentrations. Excessive ingestion of these metals by humans can cause cumulative poisoning, cancer, nervous system damage and ultimately death. This forms the basis for the increasing research with a view to remedying the levels of these heavy metals in the environment and also the growing concern by governmental agencies for the regulation of the discharge of these metals into the environment [3].

Some of the methods reported by other researchers for the removal of heavy metals from effluents include chemical precipitation or coagulation, ion exchange resin, use of commercially activated carbons, extraction and membrane processes. However, the application of these methods is often limited due to their inefficiency, high capital investment and operational costs. Consequently, there is a growing requirement for novel, efficient and effective techniques for the remediation of metal bearing waste water before their discharge into the environment. Of all these methods, adsorption onto natural adsorbents has proven to be an efficient and relatively inexpensive option for the removal of heavy metals from waste water [4-6]. Other advantages of using natural adsorbents like agricultural wastes for waste water treatment by adsorption include simple techniques, requires little or no processing, good adsorption capacity, low cost, wide spread availability and easy regeneration if required [7-8].

Nigeria is the largest producers of corn (maize) in Africa and its cobs are left in the environment during processing and after consumption. The availability of corn cobs as waste material is vast in Nigeria. The objective of this study is to investigate the potential of raw maize cob (rmc) powder as an alternative adsorbent for the removal of  $\text{Cu}^{2+}$  and  $\text{Pb}^{2+}$  from aqueous solution. Characterizations of rmc powder were done by SEM and FTIR analysis. The effect of contact time, adsorbent dose, initial dye concentration, pH and temperature were evaluated. Adsorption isotherms, kinetics, mechanism and thermodynamic parameters were also evaluated and reported.

## II. Materials and Method

### 2.1 Adsorbent Collection and Preparation

Maize cob wastes were collected from shops at new market beside Enyimba stadium Aba, in Aba South LGA of Abia state, Nigeria. The maize cob wastes were properly washed with running water from tap to remove any dirt and other particulate matter that might interact with any adsorbed metal ions. This was followed by washing with distilled water and sundried for some days. The dried samples were ground and sieved using 40 nm sieves. The samples were stored in plastic air tight containers and labelled rmc for further analysis.

### 2.2 Preparation of heavy metal solutions (Sorbate)

Stock solution of  $\text{Cu}^{2+}$  ion was prepared by weighing 3.80 g of  $\text{Cu}(\text{NO}_3)_2 \cdot 3\text{H}_2\text{O}$  into 1 litre (1000 ml) volumetric flask and made up with distilled water to have 1000 mg/L  $\text{Cu}^{2+}$  ion concentration in solution. Stock solution of  $\text{Pb}^{2+}$  ion was prepared by weighing 1.60 g of  $\text{Pb}(\text{NO}_3)_2$  into 1 litre (1000 ml) volumetric flask and made up with distilled water to have 1000 mg/L  $\text{Pb}^{2+}$  ion concentration in solution. The experimental solutions were prepared by diluting definite volume of the stock solutions to get the desired concentrations.

### 2.3 Adsorbent Characterization

Fourier transform infra-red (FTIR) spectrophotometer was used to identify the different functional groups available on the adsorbent sites and their effect on dye adsorption. The FTIR of the adsorbent was taken before adsorption using FTIR spectrophotometer (Shimadzu-8400S). 0.1 g of the adsorbent was encapsulated with 1 g of KBr spectroscopy grade (merk, Darmstadt, Germany) and by introducing the mix in a piston's cell of a hydraulic pump with compression pressure 15 KPa/cm<sup>2</sup>, the solid translucent disk was obtained which was introduced in an oven for 4hrs at 1050C to ensure the non interference of any existing water vapour or CO<sub>2</sub> molecules. The FTIR spectrum was then recorded within the wave number range 4000 – 500 cm<sup>-1</sup>. In addition, surface morphology and texture of the adsorbent was analyzed using scanning electron microscope (SEM) (Model-PHENOM ProX). Prior to scanning, some quantity of the adsorbent was placed on a double adhesive sticker placed in a sputter machine for 5 sec; this gave the adsorbent a conductive property. Sample (adsorbent) stud was fixed on a charge reduction sample holder, and then was charged in the SEM machine.

### 2.4 Batch Adsorption Experiments

Batch adsorption of  $\text{Cu}^{2+}$  and  $\text{Pb}^{2+}$  onto the adsorbent (rmc) was conducted in a 250 ml airtight Erlenmeyer flask containing 100 ml of known concentration of the heavy metals solution and an accurately weighed amount of the adsorbent. The mixtures in the flasks were agitated on a mechanical shaker operating at a constant speed of 150 rpm. The effect of contact time (15, 30, 45, 60, 75, 90, 105, 120, 135 & 150 min), adsorbent dosage (2, 4, 6, 8 & 10 g/L), initial heavy metals concentration (50, 100, 150, 200 & 250 mg/L), pH (2, 4, 6, 8, 10 & 12) and temperature (293, 303, 313, 323, 333 & 343 K) were evaluated. The flask containing the samples were withdrawn from the shaker at predetermined time intervals, filtered and the final concentrations of  $\text{Cu}^{2+}$  and  $\text{Pb}^{2+}$  in the supernatant solutions were analyzed using the Atomic absorption spectrophotometer (AAS) (Model Perkin Elmer A Analyst 200). The pH of the solution was adjusted using 1M HCl or NaOH. The amount of heavy metal uptake by the adsorbent was evaluated using:

$$\% \text{ Removal} = \left( \frac{C_0 - C_e}{C_0} \right) \times 100 \% \quad (1)$$

$$q_e = \left( \frac{C_0 - C_e}{w} \right) V \quad (2)$$

where  $C_0$  and  $C_e$  are initial and equilibrium (final) concentrations of heavy metal ions respectively.  $V$  is the volume (L) of experimental solution and  $w$  is the mass (g) of the adsorbent used.

### III. THEORY

#### 3.1. Adsorption Isotherm

The different adsorption isotherm models applied in the present study to describe the sorption equilibrium include Langmuir, Freundlich, Harkins and Jura, Dubinin–Raduskevich (D–R), Halsey, and Temkin isotherm models.

##### 3.1.1. Langmuir Isotherm

The Langmuir model describes the monolayer adsorption. It assumes a uniform energy of adsorption, a single (homogenous) layer of adsorbed solute at a constant temperature [9, 10]. The linear form of Langmuir equation is given as

$$\frac{C_e}{q_e} = \frac{1}{q_{\max} K_L} + \frac{1}{q_{\max}} C_e \quad (3)$$

where  $q_{\max}$  is the maximum metal ions uptake per unit mass of adsorbent (mg/g), which is related to the adsorption capacity,  $K_L$  is Langmuir adsorption constant (L/mg) and is related to the measure of affinity of adsorbate for the adsorbent,  $C_e$  is the metal ion residual concentration in solution,  $q_e$  is equilibrium metal ion concentration on the adsorbent (mg/g). To confirm the favourability of an adsorption process to Langmuir isotherm, the essential features of the isotherm can be expressed in terms of a dimensionless constant called separation factor or parameter  $R_L$  which can be calculated as

$$R_L = \frac{1}{1 + K_L C_0} \quad (4)$$

Where  $C_0$  is the highest initial adsorbate concentration (mg/g). The value of  $R_L$  indicates whether the isotherm is irreversible ( $R_L=0$ ), favourable ( $0 < R_L < 1$ ), linear ( $R_L = 1$ ) or unfavourable ( $R_L > 1$ ) [11].

##### 3.1.2. Freundlich Isotherm

Freundlich isotherm gives the relationship between equilibrium liquid and solid phase capacity based on the multilayer adsorption representing heterogeneous surface properties. This isotherm is based on the assumption that the adsorption sites are distributed exponentially with respect to the heat of adsorption and can be linearised as

$$\text{Log } q_e = \text{Log } K_f + \frac{1}{n} \text{Log } C_e \quad (5)$$

Where  $q_e$  = solid phase concentration in equilibrium,  $C_e$  = liquid phase metal ion concentration at equilibrium,  $\frac{1}{n}$  = intensity adsorption (heterogeneity factor),  $K_f$  = Freundlich constant (multilayer adsorption capacity). The magnitude of  $n$  gives an indication of the favourability of adsorption. It is generally stated that the value of  $n$  in the range 2-10 represent good, 1-2 moderately good and less than 1 poor adsorption characteristics [12].

##### 3.1.3. Harkins and Jura Isotherm

The Harkins and Jura isotherm can be expressed as [13, 14]

$$\frac{1}{q_e^2} = \frac{B}{A} - \frac{1}{A} \text{Log } C_e \quad (6)$$

The isotherm equation accounts for multilayer adsorption and can be explained by the existence of a heterogenous pore distribution. The Harkins-Jura isotherm parameters were obtained from the plots of  $\frac{1}{q_e^2}$  against  $\text{log } C_e$ .

##### 3.1.4. Halsey isotherm

Halsey proposed an expression for condensation of a multilayer at a relatively large distance from the surface [15] which can be linearised as:

$$\ln q_e = \frac{1}{n_H} \ln K_H - \frac{1}{n_H} \ln C_e \quad (7)$$

This equation is suitable for multilayer adsorption. A plot of  $\ln q_e$  versus  $\ln C_e$  yields slope and intercept which corresponds to  $-\frac{1}{n_H}$  and  $\frac{1}{n_H} \ln K_H$  respectively.

### 3.1.5. Temkin Isotherm

Temkin and Pyzhev [16] studied the heat of adsorption and the adsorbent-adsorbate interaction on the surfaces. The linear form of Temkin isotherm equation is given as

$$q_e = B \ln K_T + B \ln C_e \quad (8)$$

Where  $B = \frac{RT}{b}$ ,  $T$  (K) is the absolute temperature,  $R$  is the universal gas constant (8.314 J/mol),  $K_T$  is the equilibrium binding constant or adsorption potential (L/mg),  $q_e$  (mg/L) and  $C_e$  (mg/L) are the amount of adsorbed at equilibrium and equilibrium concentration respectively, and  $B$  is related to the heat of adsorption (kJ/mol).

### 3.1.6. Dubinin-Radushkevich (D-R) Isotherm

Characteristics of adsorption can also be studied by applying the Dubinin- Radushkevich (D-R) model whose linear form is written as [17]:

$$\ln q_e = \ln q_m - \beta \epsilon^2 \quad (9)$$

Where  $q_m$  = maximum adsorption capacity (mg/g),  $\beta$  = activity coefficient ( $\text{mol}^2/\text{J}^2$ )

$R$  = gas constant (8.314 J/mol/K),  $T$  = temperature in Kelvin (K),

$\epsilon$  = Polanyi or adsorptive potential.

$$\epsilon = RT \ln \left( 1 + \frac{1}{C_e} \right) \quad (10)$$

$\beta$  was further used to calculate the mean free adsorption energy  $E$  (kJ/mol) using the equation

$$E = \frac{1}{\sqrt{2} \beta} \quad (11)$$

## 3.2. Adsorption Kinetics

The pseudo-first-order, pseudo-second-order, power function, Elovich, intraparticle and Film diffusion together with Boyd kinetic models

### 3.2.1. The Pseudo-First-Order Model

The simplified linear form of pseudo first order kinetic equation of Lagergren model based on equilibrium adsorption is expressed as

$$\text{Log}(q_e - q_t) = -\frac{k_1 t}{2.303} + \text{Log } q_e \quad (12)$$

### 3.2.1. Pseudo-Second-Order Kinetic Model

This can be linearised and expressed as Ho pseudo second order equation [18]

$$\frac{t}{q_t} = \frac{1}{q_e} t + \frac{1}{q_e^2 k_2} \quad (13)$$

Here  $k_2$  is the rate constant (min g/mg) of second order adsorption. The linear plot of  $\frac{t}{q_t}$  versus  $t$  gave  $\frac{1}{q_e}$  as slope and  $\frac{1}{q_e^2 k_2}$  as intercept for adsorption of  $\text{Cu}^{2+}$  and  $\text{Pb}^{2+}$  ions onto the two adsorbent.

The initial sorption rate as is given as:

$$h = q_e^2 k_2 \quad (14)$$

Thus the rate constant  $k_2$ , initial sorption rate  $h$ , and predicted  $q_e$  can be calculated from the plot of  $\frac{t}{q_t}$  versus time  $t$ .

Among these models, the criterion for their applicability is based on judgment on the respective correlation coefficient ( $R^2$ ) and agreement between experimental and calculated value of  $q_e$  [19-21].

### 3.2.3. Elovich Kinetic Model

The Elovich equation is generally given by [22]:

$$q_t = \frac{1}{\beta} \ln(\alpha\beta) + \frac{1}{\beta} \ln t \quad (15)$$

Where  $\alpha$  is the initial adsorption rate (mg/g) and  $\beta$  is the rate constant (mg/g/min) during any one experiment. A plot of  $q_t$  versus  $\ln t$  yield a linear relationship with a slope of  $\frac{1}{\beta}$  and intersect of  $\frac{1}{\beta} \ln(\alpha\beta)$  if the sorption process fits the Elovich equation.

### 3.2.4. Power Function Kinetic Model

Equation of power function is given by

$$\log q_t = b \log t + \log a \quad (16)$$

Where  $a$  is initial rate and  $b$  is the rate constant. A plot of  $\log q_t$  versus  $\log t$  yield a straight line graph with a slope of  $b$  and intercept of  $\log a$

### 3.2.5. Intra-Particle Diffusion Model

The basic assumption with intra-particle diffusion model is that film diffusion is negligible and intra-particle diffusion is the rate determining step [23]. According to Weber and Morris [24], if the rate limiting step is the intra-particle diffusion, then the amount adsorbed at any time  $t$  should be directly proportional to the square root of contact time  $t$  and shall pass through the origin. This is defined mathematically as

$$q_t = K_{id} t^{0.5} \quad (17)$$

Where  $q_t$  (mg/g) is the amount adsorbed at time  $t$  (min.) and  $k_{id}$  (mg/g/min<sup>0.5</sup>) is the intra-particle rate constant. The Weber and Morris plots (Figure not shown) are not linear, this suggest that the rate determining step is not governed by intra-particle diffusion. The slope of the plot gives  $K_{id}$  while the intercept is  $C$ , the boundary layer effect. The larger the intercept observed, the greater will be the contribution of the surface sorption in the rate controlling step.

Due to the double nature of intra-particle diffusion (both film and pore diffusion), and in order to determine the actual rate controlling step involved in the adsorption process, the kinetic data were further analysed by using

### 3.2.6 Boyd kinetic equation [25] represented as

$$F = \frac{6}{\pi^2} \exp(-Bt) \quad (18)$$

$$\text{and } F = \frac{q}{q_e} \quad (19)$$

Where  $q_e$  is the amount of metal ion adsorbed at equilibrium (mg/g) and  $q$  represents the amount of metal ion adsorbed at any time  $t$  (min),  $F$  represent the fraction of metal ion adsorbed at any time  $t$ , and  $Bt$  is the mathematical function of  $F$ . Equation 18 can be rearranged and given by

$$Bt = -0.4977 - \ln(1-F) \quad (20)$$

### 3.3. Thermodynamic Parameters

Gibb's free energy and Van't Hoff equations were used to study the effect of adsorption of metal ions ( $\text{Cu}^{2+}$  and  $\text{Pb}^{2+}$ ) on the raw maize cob. The free energy change  $\Delta G$ , enthalpy change  $\Delta H$  and entropy change  $\Delta S$  was determined by assuming that the activity coefficients are unity at low concentration (in the Henry's law sense), the apparent equilibrium constant  $K'_c$  of the biosorption is defined as [26, 27]:

$$K'_c = \frac{C_{ad,e}}{C_e} = \frac{C_o - C_e}{C_e} \quad (21)$$

Where  $C_o$  = initial metal ion concentration,  $C_{ad,e}$  = the metal ion concentration on the adsorbent at equilibrium and  $C_e$  = concentration of the metal ion at equilibrium.

The  $K'_c$  value is used in the equation below to determined the Gibb's free energy  $\Delta G$  of biosorption

$$\Delta G = -RT \ln K'_c \quad (22)$$

The Gibbs free energy equation is given by:

$$\Delta G = \Delta H - T\Delta S \quad (23)$$

Combining equations (22) and (23) and rearranging, we obtain the Van't Hoff equation;

$$\ln K'_c = \left\{ -\frac{\Delta H}{R} \right\} \frac{1}{T} + \frac{\Delta S}{R} \quad (24)$$

The enthalpy change  $\Delta H$  and the entropy change  $\Delta S$  can be obtained from the slope and intercept of the Gibbs plot of  $\Delta G$  against  $T$ .

Where:  $R$  is gas constant (8.314Jmol<sup>-1</sup>K<sup>-1</sup>) and  $T$  is absolute temperature in Kelvin.

### III. RESULTS AND DISCUSSION

#### 4.1 Adsorbent Characterization

The FTIR spectra of raw maize cobs, rmc were obtained using KBr pellets within the spectral range of 4000-400  $\text{cm}^{-1}$  and is shown in Fig. 1. It shows the FTIR spectrum of raw maize cob with the functional groups responsible for the metal ion coordination. The peaks 419.53  $\text{cm}^{-1}$  and 526.58  $\text{cm}^{-1}$  represent the carbon-halogen (C-X) bond. Peaks at 1039.67 and 1190.12  $\text{cm}^{-1}$  are due to C-O stretch from alcohol and C-N from aliphatic amine. Peaks at 1511.28  $\text{cm}^{-1}$  show N-O symmetric from nitro compounds. C=C stretch is responsible for the peak at 1654.01  $\text{cm}^{-1}$ . Sharp peaks at 2265.47  $\text{cm}^{-1}$  represents C=C stretch from alkyne. C≡N stretch from nitriles is responsible for the peak at 2376.38  $\text{cm}^{-1}$ . The peaks at 3257.88  $\text{cm}^{-1}$ , 3529.85  $\text{cm}^{-1}$  and 3742.03  $\text{cm}^{-1}$  are due to O-H stretching (from alcohols and carboxylic acids) and N-H symmetric and asymmetric stretch from amines and amides respectively. O-H from adsorbed water on the surface is responsible for the peak at 3857.76  $\text{cm}^{-1}$ .

Furthermore, Fig. 2 shows the SEM images of rmc powder. It can be observed from 1000 magnification in Fig. 2a that the surface of RCC powder is rough and uneven. On further magnification (10000) as indicated in Fig. 2b, the surface is very irregular and contains some pores.

#### FTIR- 8400S FOURIER TRANSFORM INFRARED SPECTROPHOTOMETER

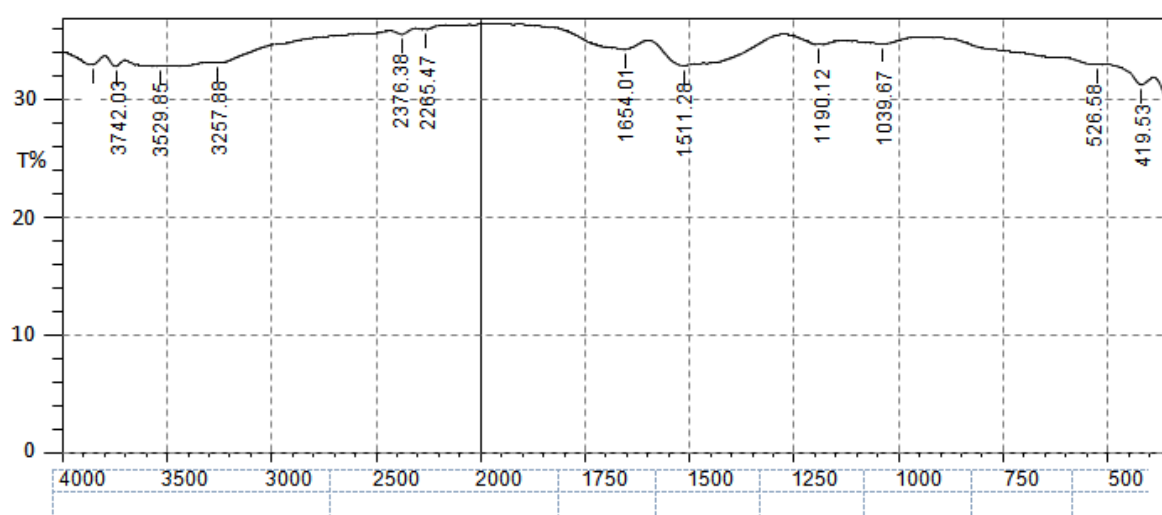


Fig. 1: FTIR spectra of rmc powder

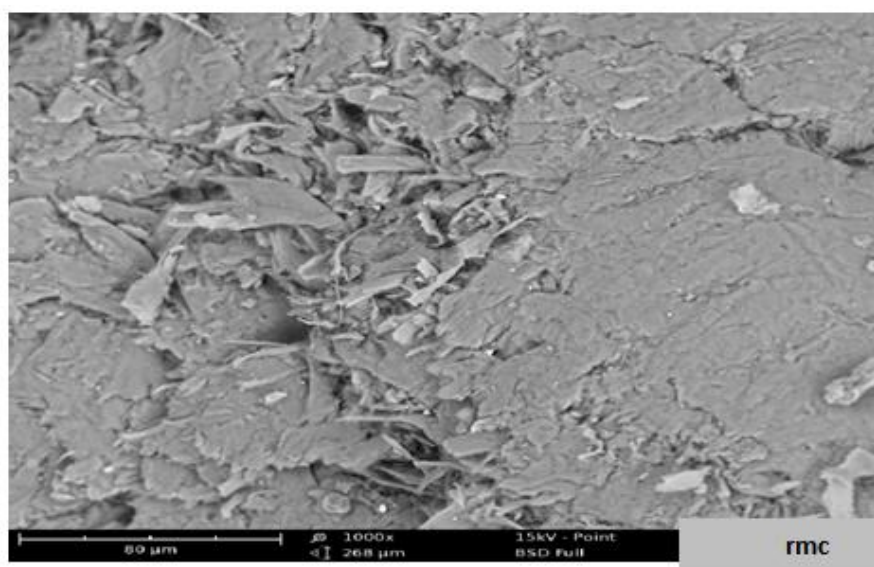


Fig. 2a: SEM image of raw maize cob at 1000x

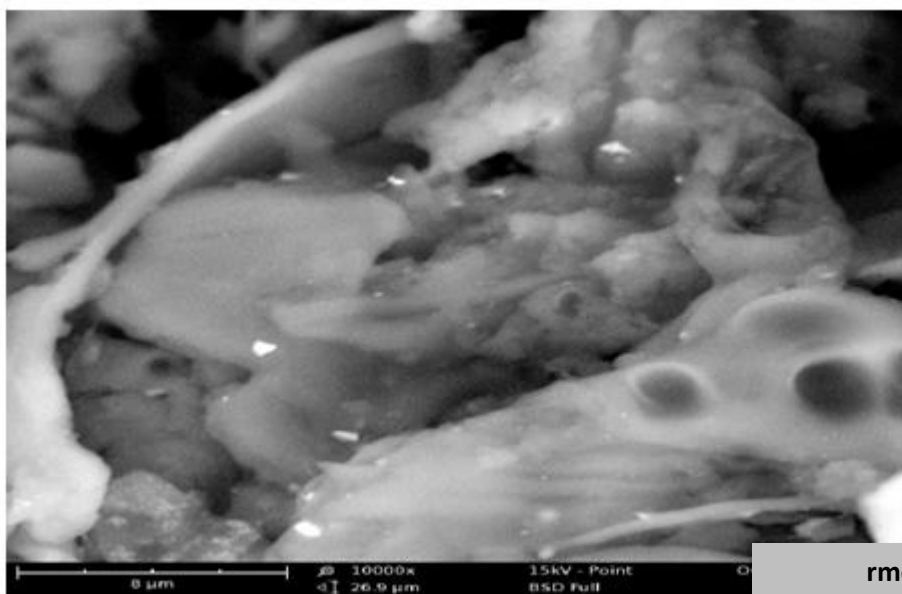


Fig. 2b: SEM image of raw maize cob at 10000x

4.2 Effect of Contact Time

The time taken to attain equilibrium for  $\text{Cu}^{2+}$  and  $\text{Pb}^{2+}$  at neutral pH, temperature of  $27^\circ\text{C}$  and moderate shaker speed at 150 rpm using 2 g of the rmc is shown in Fig 3. The percentage removal of  $\text{Pb}^{2+}$  by raw maize cob increases swiftly and attains equilibrium at 105 minutes while that of  $\text{Cu}^{2+}$  increases steadily and attains equilibrium at 75 minutes after which desorption takes place in both cases. The decrease in percentage removal of metal ion after reaching the maximum adsorption may be due to the saturation of adsorption sites of the adsorbents with the metal ions. It may also be due to the breakage of newly formed weak adsorption bonds due to constant agitation.

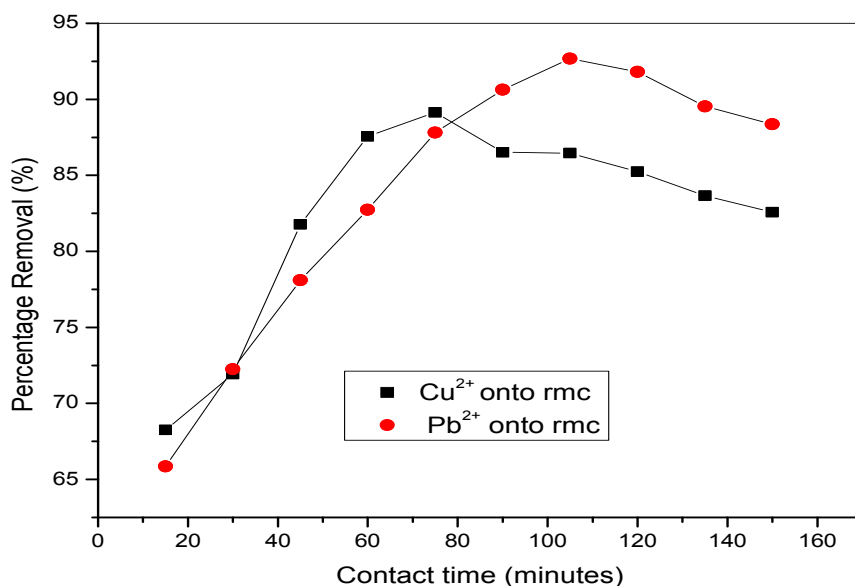


Fig. 3: Effect of contact time on adsorption of  $\text{Cu}^{2+}$  and  $\text{Pb}^{2+}$  onto raw maize cob

#### 4.3 Effect of adsorbent dosage

The effect of dosage of the adsorbent (raw maize cob) on  $\text{Cu}^{2+}$  and  $\text{Pb}^{2+}$  at neutral pH, temperature of  $27^\circ\text{C}$  and moderate shaker speed at 150 rpm and 100 mg/L of metals concentration is shown in Fig. 4. It can be inferred that percentage removal for both metal ions increases with increase in adsorbent dosage from 2 g to 10 g. The increase in  $\text{Cu}^{2+}$  and  $\text{Pb}^{2+}$  percentage removal with increase in adsorbent dose is due to the greater availability of the exchangeable sites and functional groups at higher dosage. These functional groups were important in the formation of Van der waals bonding which play a major role in binding metals to the adsorbent during adsorption process [28]. Because of increase in the adsorbent dosage, the amount of metal ions adsorbed per unit mass ( $q_e$ ) decreases in both cases.

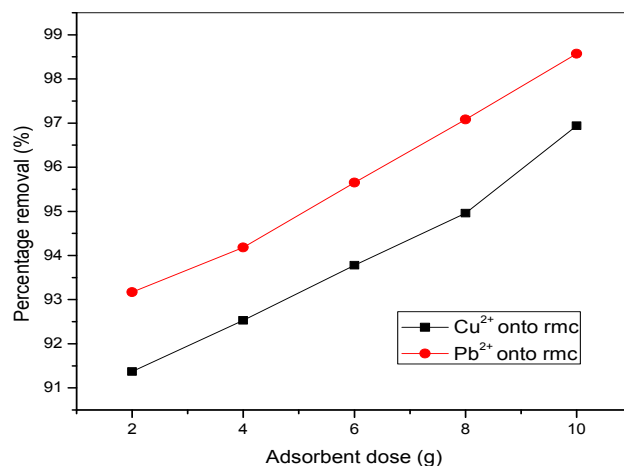


Fig. 4: Effect of adsorbent dosage rmc on percentage removal of  $\text{Cu}^{2+}$  and  $\text{Pb}^{2+}$

#### 4.4 Effect of initial concentration of adsorbate

The effect of initial concentration of adsorbate ( $\text{Cu}^{2+}$  and  $\text{Pb}^{2+}$ ) on the adsorbent (rmc) is shown in Fig. 5. The amount of metal ion adsorbed increased with increase in initial metal ion concentration. For an increase in initial concentration of metal ions from 50 mg/L to 250 mg/L, the amount of  $\text{Cu}^{2+}$  adsorbed increases from 2.38 mg/g to 10.23 mg/g while for  $\text{Pb}^{2+}$  it increases from 2.41 mg/g to 10.42 mg/g. The increase in amount of metal ions adsorbed (adsorption capacity) is due to the higher adsorption rate and the utilization of active sites available for the adsorption at higher concentration [29].

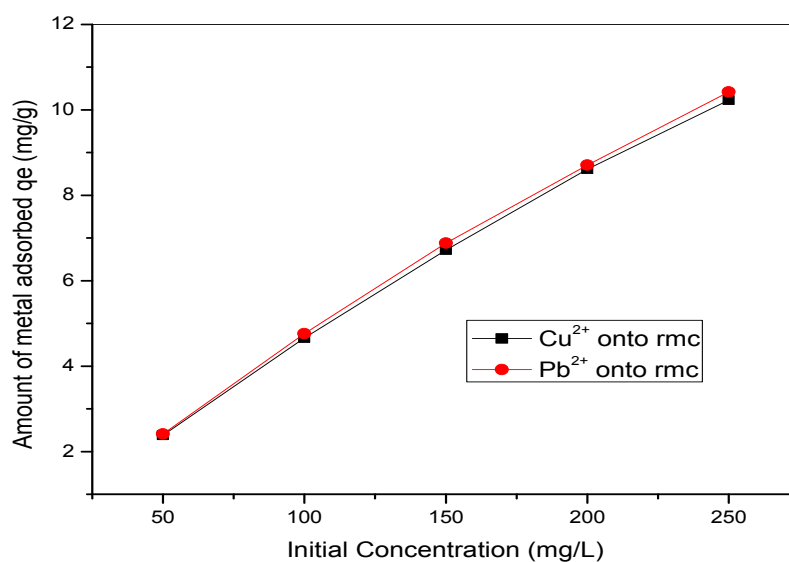


Fig. 5: Effect of initial concentration of  $\text{Cu}^{2+}$  and  $\text{Pb}^{2+}$  onto rmc

#### 4.5 Effect of pH

The effects of pH on the adsorption of  $\text{Cu}^{2+}$  and  $\text{Pb}^{2+}$  onto the adsorbent (rmc) are shown in Fig. 6. The percentage removal of  $\text{Cu}^{2+}$  and  $\text{Pb}^{2+}$  for the adsorbent (rmc) increases with increasing pH from 2 to 12. This is because at lower pH, the overall surface charge on the adsorbent will be positive, which will inhibit the approach of positively charged metal cations, consequently reducing metal ion binding on the adsorbent surface. At higher pH, the adsorbent surface is negatively charged thereby encouraging more metal ion uptake due to the electrostatic forces of attraction between the negatively charged adsorbent surface and the positively charged metal ion. These results are in agreement with what has been reported in literature [1, 30, 31].

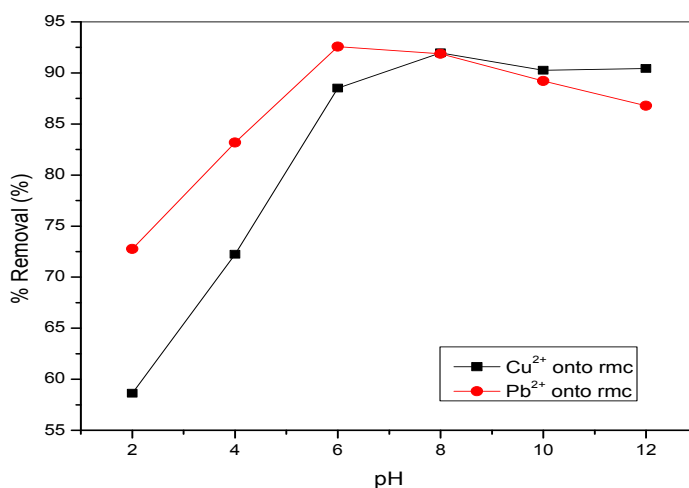


Fig.6: Effect of pH on the adsorption of  $\text{Cu}^{2+}$  and  $\text{Pb}^{2+}$  onto rmc

#### 4.6. Effect of Temperature

The effect of temperature on the adsorption of metal ions onto the adsorbent is shown in Fig.7. The percentage removal of  $\text{Cu}^{2+}$  increased with increase in temperature, while the percentage removal of  $\text{Pb}^{2+}$  decreased with increase in temperature. The increase in percentage removal of  $\text{Cu}^{2+}$  with increase in temperature is as a result of widening of pores on the active sites of the adsorbent which create more room for greater adsorption. In addition, this increase in adsorption with temperature may also be due to the increase in number of active adsorption sites generated as a result of breaking of some internal bonds near the edge of active sites in the adsorbents [32]. Whereas the decrease in percentage removal of  $\text{Pb}^{2+}$  at higher temperature may be due to the damage of active binding sites in the biomass [33].

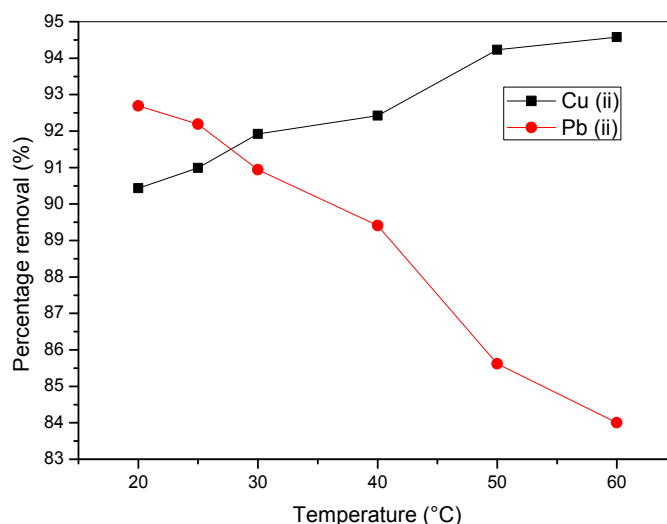
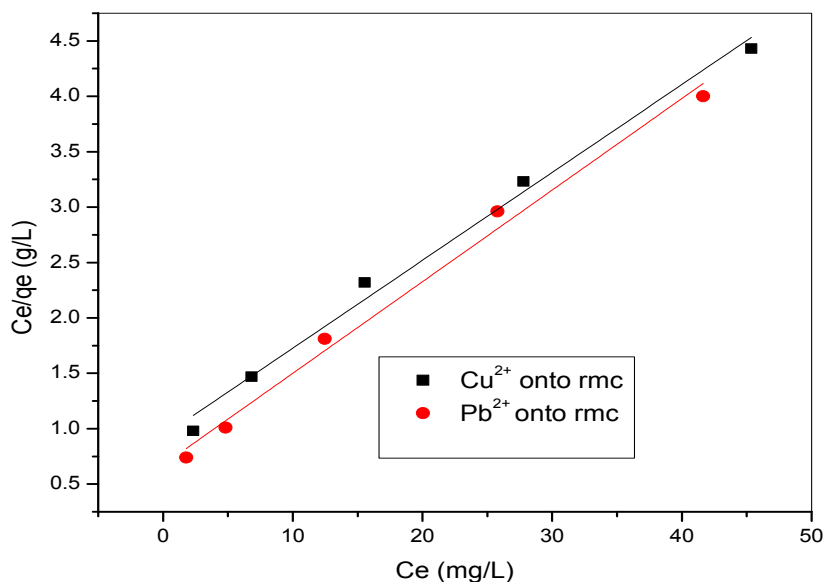


Fig. 7: Effect of temperature on percentage removal of  $\text{Cu}^{2+}$  and  $\text{Pb}^{2+}$  by raw maize cob

#### 4.7. Adsorption Isotherms

Six adsorption isotherm models were applied to describe the relationship between the heavy metals ( $\text{Cu}^{2+}$  and  $\text{Pb}^{2+}$ ) concentration in the bulk solution and that on the rmc powder surface namely: the Langmuir, Freundlich, Harkins and Jura, Dubinin–Raduskevich (D–R), Halsey, and Temkin isotherm models. The plots of the various isotherms are illustrated in Figures 8- 11. The values obtained from the intercepts and slopes for the various plots are summarized in Table 1.



**Fig. 8:** Langmuir adsorption isotherm of  $\text{Cu}^{2+}$  and  $\text{Pb}^{2+}$  onto rmc

It is evident from the linear plots in Fig.8 and the values of correlation coefficient in Table 1 that the experimental data fitted well to the Langmuir Isotherm model for the adsorption of both heavy metals. In addition, the  $R_L$  values of  $\text{Cu}^{2+}$  and  $\text{Pb}^{2+}$  adsorption onto rmc are between 0 and 1, which confirms the favourability of the adsorption process to Langmuir isotherm.

The Freundlich isotherm model plot for the adsorption of  $\text{Cu}^{2+}$  and  $\text{Pb}^{2+}$  onto rmc is shown in Fig. 9. It is evident from the plot and the values of correlation coefficient (in Table 1) that the experimental data also fitted well to the Freundlich isotherm model. In addition, the  $K_f$  values obtained from the Freundlich model suggest that the metal binding affinity was in the order  $\text{Pb}^{2+}$  onto rmc >  $\text{Cu}^{2+}$  onto rmc. Also, the adsorption intensities  $n$  (Table 1) were found to be in the order of  $\text{Pb}^{2+}$  onto rmc >  $\text{Cu}^{2+}$  onto rmc. The higher value of  $K_f$  indicates higher adsorption capacity for metal ions and the values of  $n$  which lies between 1-10 indicating favourable adsorption to the Freundlich isotherm [34, 35].

The Halsey isotherm plot for  $\text{Cu}^{2+}$  and  $\text{Pb}^{2+}$  ions onto the raw maize cob powder (rmc) is represented in Fig. 10 and the relevant isotherm parameters are calculated and presented in Table 1. The linearity and values of correlation coefficient reflects the adequacy of Temkin model in explaining the adsorption of  $\text{Cu}^{2+}$  and  $\text{Pb}^{2+}$  ions onto the raw maize cob powder (rmc). The fitting of the experimental data to Halsey isotherm equation verifies the heteroporous nature of the rmc adsorbent.

The Temkin isotherm model for the adsorption of  $\text{Cu}^{2+}$  and  $\text{Pb}^{2+}$  ions onto the raw maize cob powder (rmc) is represented in Fig. 11 and the Temkin parameters are calculated and summarized in Table 1. It can be observed from Table 1, that the Temkin model also gave a good fitting for the adsorption of  $\text{Cu}^{2+}$  and  $\text{Pb}^{2+}$  ions onto rmc powder. This reflects the efficiency of Temkin model in explaining the adsorption process.

The the Harkins and Jura isotherm, and the Dubinin – Radushkevich plots (Figures not shown) were not found efficient in the description of the adsorption of  $\text{Cu}^{2+}$  and  $\text{Pb}^{2+}$  ions onto the raw maize cob powder (rmc). However, the specific model parameters and correlation coefficient were calculated and included in Table 1.

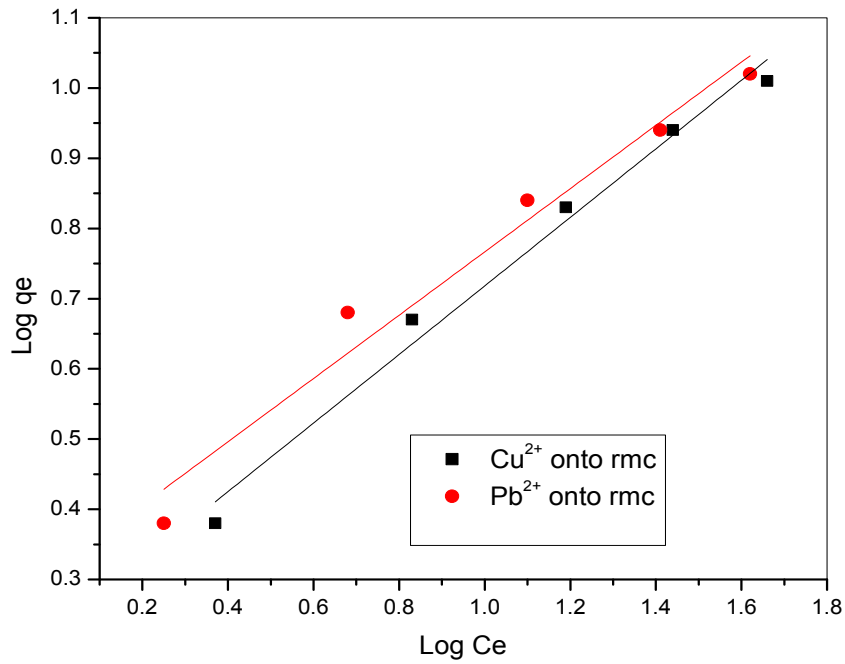


Fig. 9: Freundlich isotherm plot for adsorption of Cu<sup>2+</sup> and Pb<sup>2+</sup> onto rmc

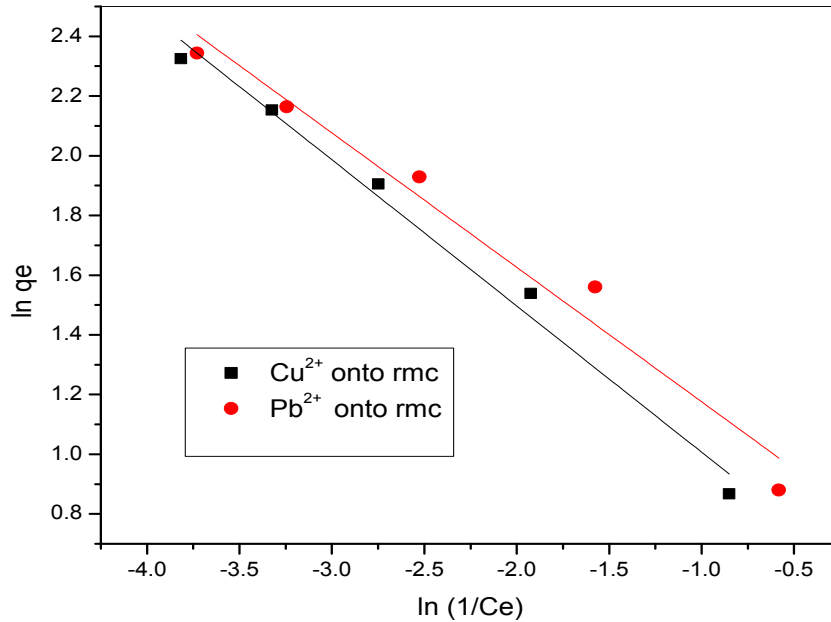


Fig. 10: Halsey isotherm plot for adsorption of Cu<sup>2+</sup> and Pb<sup>2+</sup> onto rmc

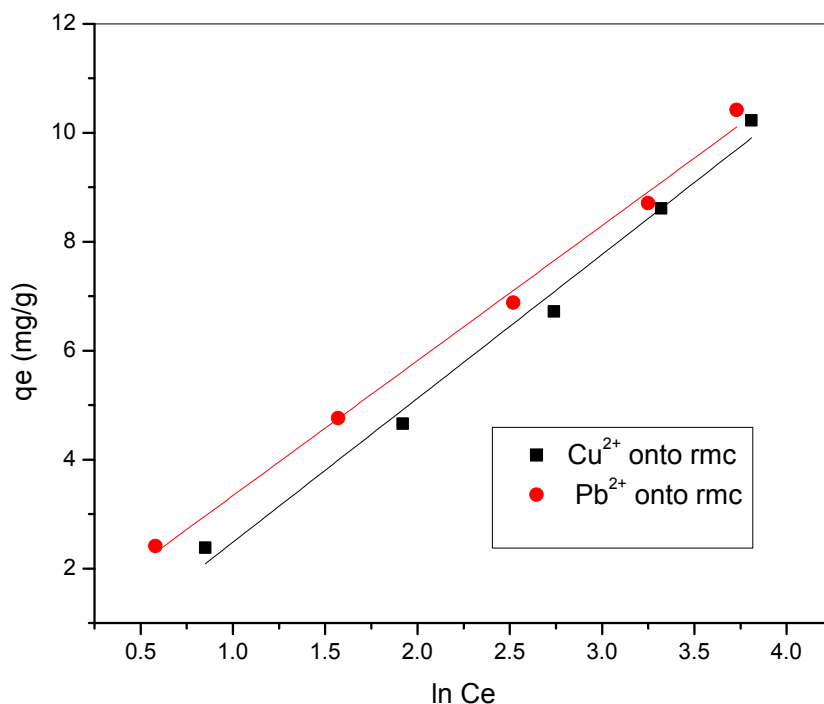


Fig. 11: Temkin isotherm plot of Cu<sup>2+</sup> and Pb<sup>2+</sup> onto rmc

Table 1: The Isotherm Parameters and Values of Correlation Coefficient for the Adsorption of Cu<sup>2+</sup> and Pb<sup>2+</sup> by rmc

	<b>q<sub>max</sub></b> (mg/g)	<b>K<sub>L</sub></b> (Lg <sup>-1</sup> )	<b>R<sup>2</sup></b>
<b>Langmuir</b>			
Cu <sup>2+</sup>	12.658	0.085	0.992
Pb <sup>2+</sup>	12.195	0.122	0.992
<b>Freundlich</b>	<b>K<sub>f</sub></b> (mg/g)(L/mg) <sup>1/n</sup>	<b>n</b>	<b>R<sup>2</sup></b>
Cu <sup>2+</sup>	1.694	2.049	0.986
Pb <sup>2+</sup>	2.065	2.222	0.976
<b>Halsey</b>	<b>n<sub>H</sub></b>	<b>K<sub>H</sub></b>	<b>R<sup>2</sup></b>
Cu <sup>2+</sup>	2.07	3.03	0.990
Pb <sup>2+</sup>	2.22	5.00	0.977
<b>Temkin</b>	<b>B</b> (kJ/mol)	<b>K<sub>T</sub></b> (L/g)	<b>R<sup>2</sup></b>
Cu <sup>2+</sup>	2.641	0.942	0.990
Pb <sup>2+</sup>	2.479	1.413	0.994
<b>Harkins and Jura</b>	<b>A</b>	<b>B</b>	<b>R<sup>2</sup></b>
Cu <sup>2+</sup>	8.130	1.537	0.807
Pb <sup>2+</sup>	9.259	1.491	0.768
<b>D.R</b>	<b>q<sub>m</sub></b> (mg/g)	<b>E</b> (kJ/mol)	<b>R<sup>2</sup></b>
Cu <sup>2+</sup>	7.78	0.500	0.839
Pb <sup>2+</sup>	8.01	0.707	0.863

#### 4.8. Adsorption Kinetics

Five kinetic models i.e., pseudo-first-order, pseudo-second-order, power function, Elovich and Intraparticle / Film diffusion models were applied to investigate the kinetics and potential rate determining steps of the adsorption of Cu<sup>2+</sup> and Pb<sup>2+</sup> ions onto raw maize cob (rmc) powder.

The pseudo-first-order model did not provide a good fit to the experimental data as seen in the low values of correlation coefficient (Table 2) and poor linearity of log (q<sub>e</sub> - q<sub>t</sub>) versus t (Figure not shown). In

addition, the theoretical and experimental equilibrium adsorption capacity  $q_e$  obtained from the plot varied widely, confirming the inadequacy of the pseudo-first-order model for describing the adsorption kinetics of  $\text{Cu}^{2+}$  and  $\text{Pb}^{2+}$  ions onto raw maize cob (rmc) powder.

The pseudo-second-order model provided excellent linearity with high values of correlation coefficients,  $R^2$  (Table 2) as shown in the plot of  $t/qt$  against  $t$  in Fig.12. In addition, there was good agreement between the calculated  $q_e$  and the experimental  $q_e$  values indicating that the adsorption of  $\text{Cu}^{2+}$  and  $\text{Pb}^{2+}$  ions onto raw maize cob (rmc) powder followed the pseudo-second-order kinetics. This suggests that the metal uptake process is due to chemisorptions and such chemical sorption occurs by the polar functional groups of lignin which include functional groups of alcohols, aldehydes, ketones, acids, phenolic hydroxides and ethers as chemical bonding agents [36, 37].

The power function model and the Elovich model showed inadequacy in providing a good fitting to the experimental data as seen by their poor values of linear regression in Table 3 (Figure not shown). The power function constants,  $a$ ,  $b$  and that of the Elovich model values of  $\alpha$  and  $\beta$  including their correlation coefficients,  $R^2$  are given in Table 3.

The intra-particle diffusion (Weber Morris) model was evaluated to identify the adsorption mechanism. The Weber Morris constant,  $K_{id}$  and  $C$  are given in Table 3. The Weber Morris plot for the adsorption of  $\text{Cu}^{2+}$  and  $\text{Pb}^{2+}$  ions onto raw maize cob (rmc) powder (figure not shown) was highly non linear and did not pass through the origin suggesting that intra-particle diffusion was not the only rate limiting step, some other mechanism along with intra-particle diffusion is involved.

Furthermore, due to the double nature of intra-particle diffusion (both film and pore diffusion), and in order to determine the actual rate controlling step involved in the adsorption process, the kinetic data were further analysed by using Boyd kinetic equation. A straight line passing through the origin is an indication of adsorption processes governed by particle diffusion mechanism; otherwise they are governed by film diffusion [38]. As can be seen from Fig. 13, Boyd plots of the rmc for the  $\text{Cu}^{2+}$  and  $\text{Pb}^{2+}$  adsorption data were neither linear nor passes through the origin. This indicates that film diffusion is the rate limiting step for the adsorption of  $\text{Cu}^{2+}$  and  $\text{Pb}^{2+}$  ions onto rmc.

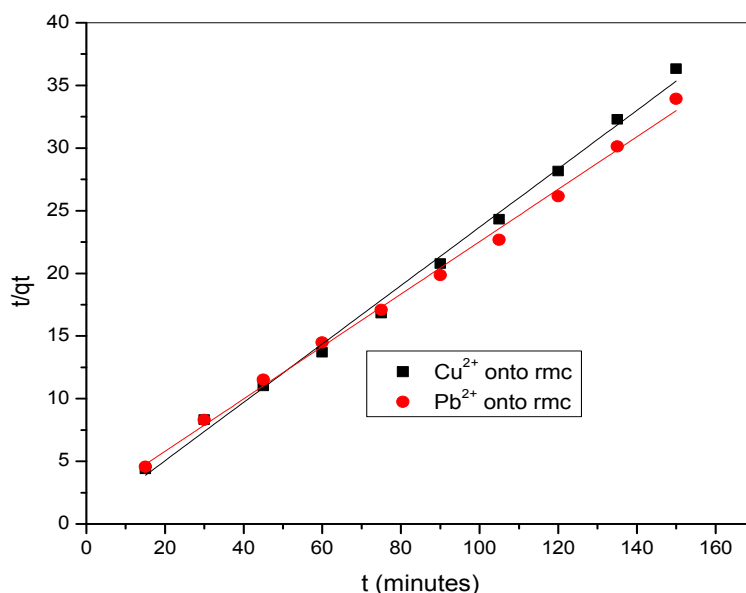


Fig. 12: Pseudo-second order plot for adsorption of  $\text{Cu}^{2+}$  and  $\text{Pb}^{2+}$  onto rmc

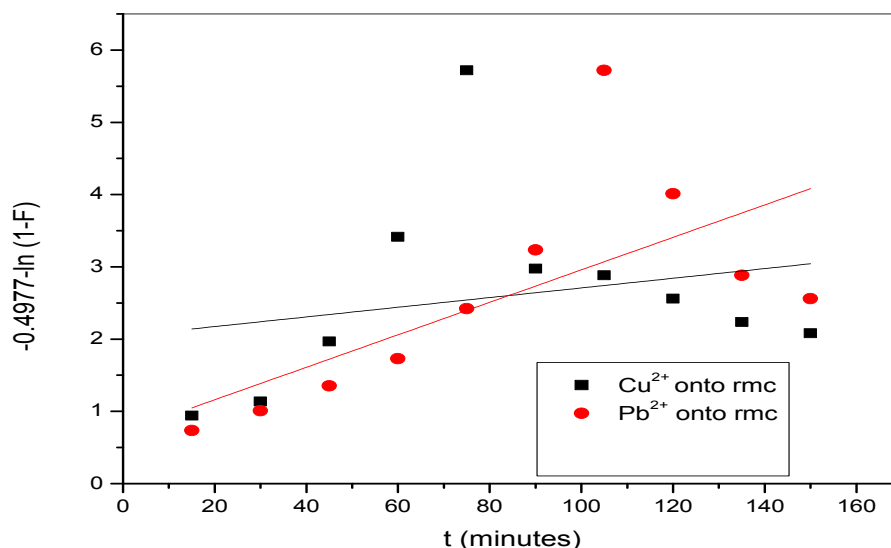


Fig. 13: A Boyd plot of adsorption of Cu<sup>2+</sup> and Pb<sup>2+</sup> onto rmc

Table 2: Pseudo-first and second order kinetic model parameters, equilibrium adsorption capacity and values of correlation coefficient for Cu<sup>2+</sup> and Pb<sup>2+</sup> adsorption onto rmc

Heavy metals	Pseudo-First Order Model				Pseudo-Second Order Model			
	qe (exp) (mg/g)	k <sub>1</sub> (g.mg <sup>-1</sup> min <sup>-1</sup> )	qe (cal) (mg/g)	R <sup>2</sup>	h(mg.g <sup>-1</sup> min <sup>-1</sup> )	K <sub>2</sub> (g.mg <sup>-1</sup> min <sup>-1</sup> )	qe (cal) (mg/g)	R <sup>2</sup>
Cu <sup>2+</sup>	4.47	5 x10 <sup>-3</sup>	0.360	0.054	2.577	0.139	4.29	0.996
Pb <sup>2+</sup>	4.64	2.07 x10 <sup>-2</sup>	1.377	0.033	0.620	0.027	4.55	0.999

Table 3: Elovich, Power function, Intra-particle and Boyd kinetic model parameters with their values of correlation coefficient for Cu<sup>2+</sup> and Pb<sup>2+</sup> adsorption onto rmc powder

Power Function	A (g.mg <sup>-1</sup> min <sup>-1</sup> )	B (g.mg <sup>-1</sup> min <sup>-1</sup> )	R <sup>2</sup>
Cu <sup>2+</sup>	4.09	0.022	0.816
Pb <sup>2+</sup>	4.48	0.008	0.370
Elovich Model	β (g.min <sup>-1</sup> )	α (mg.g.mg)	R <sup>2</sup>
Cu <sup>2+</sup>	378.14	2.710	0.618
Pb <sup>2+</sup>	10.326	1.686	0.910
Intraparticle diffusion	K <sub>id</sub> (mg/g/min <sup>0.5</sup> )	C (mg/g)	R <sup>2</sup>
Cu <sup>2+</sup>	0.087	3.358	0.482
Pb <sup>2+</sup>	0.152	2.873	0.839
Boyd model	B (min <sup>-1</sup> )	C	R <sup>2</sup>
Cu <sup>2+</sup>	0.007	2.040	0.068
Pb <sup>2+</sup>	0.023	0.711	0.456

4.9. Adsorption Thermodynamics

The enthalpy change ΔH and the entropy change ΔS can be obtained from the slope and intercept of the Gibbs plot of ΔG against T in Fig. 13. . The negative values of Gibbs free energy change ΔG at various temperatures (Table 4) suggest that the adsorption of Cu<sup>2+</sup> ion is rapid and feasible. This could be an explanation for high metal binding capacity shown by rmc. The negative value of ΔG decreases with increase in temperature, indicating the spontaneous nature of Cu<sup>2+</sup> ion adsorption and it is inversely proportional to temperature [26, 39]. The positive value of enthalpy change ΔH (Table 4) confirms the endothermic process of adsorption. This result is also supported by the increase in the value of adsorption capacity of rmc with the rise in temperature. The increasing sorption capacity of the adsorbent with temperature is due to the enlargement of pores and/or the activation of the adsorbent surface [40]. Additionally, the positive value of entropy change ΔS of adsorption of Cu<sup>2+</sup> onto rmc shows the increased degree of free active sites at the solid-liquid interface during the adsorption process.

However, for the adsorption of  $Pb^{2+}$  ions onto rmc, the negative value of  $\Delta G$  (Table 4) increases with increase in temperature. The negative values of  $\Delta H$  and entropy change  $\Delta S$  (Table 4) indicated the exothermic behaviour of the reaction. This shows that the interaction of  $Pb^{2+}$  ions onto rmc is an energetically stable exothermic process and that adsorption occurred through a bonding mechanism [41, 42]. The negative values for  $\Delta G$ ,  $\Delta H$  and  $\Delta S$  of  $Pb^{2+}$  ions confirmed that the adsorption process proceed more at lower temperature.

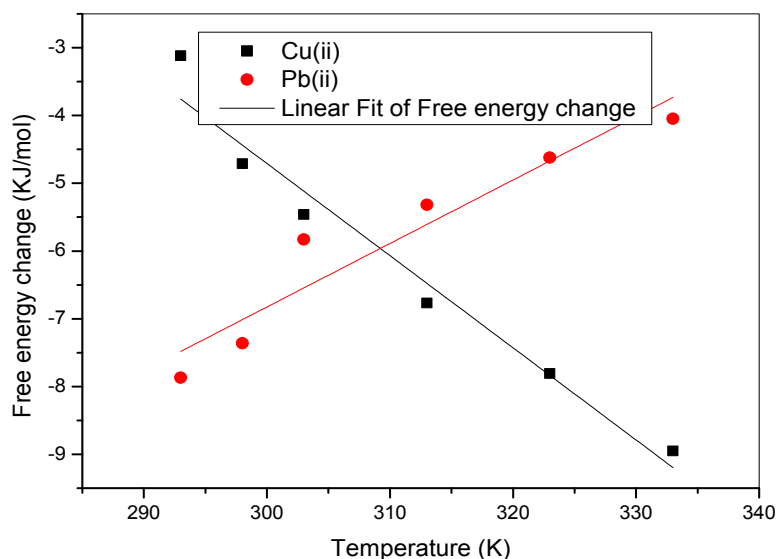


Fig. 13: Gibb's plot of adsorption of  $Cu^{2+}$  and  $Pb^{2+}$  onto rmc

Table 4: Thermodynamic parameters for the adsorption of  $Cu^{2+}$  and  $Pb^{2+}$  ions onto raw maize cob (rmc) powder

Temperature (K)	$\Delta G$ (KJ/mol)	$\Delta H$ (KJ/mol)	$\Delta S$ (J/mol. K)
<b><math>Cu^{2+}</math></b>			
293	-3.12		
303	-4.71		
313	-5.46	30.39	114.82
323	-6.77		
333	-7.81		
343	-8.95		
<b><math>Pb^{2+}</math></b>			
293	-7.87		
303	-7.36		
313	-5.83	-31.70	-81.31
323	-5.32		
333	-4.62		
343	-4.05		

#### IV. CONCLUSION

The adsorption process for the removal of heavy metal ions ( $Cu^{2+}$  and  $Pb^{2+}$ ) from aqueous solution using raw maize cob has been presented. The percentage removal as well as the amount of metal ions adsorbed was determined to be a function of contact time, temperature, pH, initial concentration and adsorbent dosage. The equilibrium amount of metals adsorbed increased with increase in initial concentration of the metal ions. On thermodynamic parameters, the negative values of Gibbs free energy  $\Delta G$  at various temperatures show that the adsorption processes were feasible. Enthalpy changes  $\Delta H$  for  $Cu^{2+}$  and  $Pb^{2+}$  adsorption are endothermic and exothermic respectively. Entropy change  $\Delta S$  of  $Cu^{2+}$  and  $Pb^{2+}$  adsorption are positive and negative respectively. It was observed that pseudo-second order kinetic model best fitted the adsorption of these two heavy metal ions onto the adsorbent. Kinetic mechanism of the adsorption process was found to be by film diffusion. Adsorption isotherms were found to be fitted to Langmuir, Temkin, Freundlich and Halsey models. FTIR and SEM analyses confirm the ionisable functional groups and rough edges at the surface of raw maize cob (rmc) which equally enhance their adsorption. It is therefore concluded that rmc can be use as an effective adsorbent for removal of heavy metals ( $Pb^{2+}$  and  $Cu^{2+}$ ) from waste water.

## References

- [1]. J. Nadia, A.M. Munawar, B. Sidra, and T. Sidra, Biosorption of Hg (II) and Cd (II) from waste water by using *Zea mays* waste, *J. Chem. Soc. Pak.*, 31(2), 2009, 362-369.
- [2]. N. Loubna, G. Iihem, H. Qualid, and C. Mahdichiha, Batch sorption dynamics and equilibrium for the removal of cadmium ions from aqueous phase wheat bran, *Journal of Hazardous Material*, 149, 2007, 115-125.
- [3]. J.M. Okuo, and A.C. Ozioko, Adsorption of Lead and Mercury ions on chemically treated periwinkle shells, *Journal chemistry Society of Nigeria*, 26(1), 2001, 60-65.
- [4]. H. Aydin, Y. Bulut and C. Yerlinkaya, Removal of copper (II) from aqueous solution by adsorption onto low-cost adsorbents, *Journal of Environmental management* 87, 2008, 37-45.
- [5]. N.A. Khan, S. Ibrahim, and P. Subramaniam, Elimination of Heavy metals from wastewater using agricultural wastes as adsorbents, *Malaysian Journal of Science*, 23, 2004, 43-51.
- [6]. S. Rafika, T. Djilali, B. Benchreit, and B. Ali, Adsorption of Heavy metals (Cd, Zn and Pb) from water using keratin powder prepared from Algerian sheep Hoofs, *European Journal of Scientific Research*, 35 (3), 2009, 416-425.
- [7]. E. Forgass, T. Eserhat, and G. Oros, Removal of synthetic dye from waste waters: A review, *Journal of Env. Intern.*, 30, 2004, 971.
- [8]. T. Robinson, G. McMillan, R. Marchant, and P. Nigam, Remediation of dyes in textile effluent: A critical review on current treatment technologies with a propose alternative, *J. Biores Tech.*, 77, 2001, 247-252.
- [9]. K. S. Bharathi, S.T. Ramesh, Removal of dyes using agricultural waste as low-cost adsorbents: A review, *Appl. Water Sci.* 3, 2013, 773 –790.
- [10]. M.A. Al-Ghouti, M.A.M Khraishch, S.J. Allen, and M.N. Ahmed, The removal of dyes from textile wastewater: a study of physical characteristics and adsorption mechanisms of diatomaceous earth, *J. Env. Manag.*, 69, 2003, 230 – 237.
- [11]. K. Kadirvelu, and C. Namasivayam, Adsorption of Cd (II) from aqueous solution using activated carbon from coconut coir pith as metal biosorbent, *Adv. Environ. Res.*, 7(2), 2003, 471-478.
- [12]. Z. Aksu, and T. Kutsal, A bioseparation process for removing Pb<sup>2+</sup> ion from waste water by using *c. vulgari*, *Journal of Chemical Technology and Biotechnology*, 52, 1991, 109-118.
- [13]. C.A. Bazar, Applicability of the various adsorption models of three dyes adsorbed onto activated carbon prepared from waste apricot, *Journal of Hazardous Materials*, B134, 2006, 232-241.
- [14]. W.D. Harkins, and C.J. Jura, The decrease of free surface energy as a basis for the development of equations for adsorption isotherms and the existence of two condensed phases in films on solids, *Journal of Chemical Physics*, 12, 1944, 112-113.
- [15]. T.F. Hassanein, and B. Koumanova, Evaluation of adsorption potential of the agricultural waste wheat straw for basic yellowish 21, *Journal of the University of Chemical Technology and Metallurgy*, 45(4), 2010, 407-414.
- [16]. M.I. Temkin, and V. Pyzchev, Kinetics of ammonia synthesis on promoted iron catalyst, *Acta. Phys. Chem. USSR*, 12, 1940, 327-356.
- [17]. P.S. Kumar, M. Palaniyappan, M. Priyadarshini, A.M. Vigensh, A. Thonjiappan, P. A.F. Sebastina, R.A. Tanvir, and R. Srinath, Adsorption of basic dye onto raw and surface-modified agricultural waste, *Env. Progress and Sustainable Energy*, 33(1), 2013, 87 – 98.
- [18]. Y.S. Ho, and G. McKay, Pseudo-second order model for sorption process, *Process. Biochem.*, 34, 1999, 451-465.
- [19]. N. Sharma, and B.K. Nnadi, Utilization of sugarcane baggase, an agricultural waste to remove malachite green dye from aqueous solution, *J. Mater. Environ. Sci.*, 4(6), 2013, 1052-1065.
- [20]. P.S. Kumar, M. Palaniyappan, M. Priyadarshini, A.M. Vigensh, A. Thonjiappan, P.A.F. Sebastina, R.A. Tanvir, and R. Srinath, Adsorption of basic dye onto raw and surface-modified agricultural waste, *Env. Progress and Sustainable Energy*, 33(1), 2013, 87 – 98.
- [21]. S. Patil, S. Renukdas, and N. Patel, Removal of methylene blue, a basic dye from aqueous solutions by adsorption using teak tree (Tectonagradnic) bark powder, *Inter. J. Env. Sci.* 1(5), 2011, 711 – 726.
- [22]. D.L. Sparks, Kinetics of reaction in pure and mixed systems in the soil physical chemistry, *Boca Raton CRC press*, 1986, 12-18.
- [23]. M.S. Venkata, S.V. Ramanaiah, and P.N. Sarma, Biosorption of direct azo dye from aqueous phase onto spirogyra sp. 102: Evaluation of kinetics and mechanistic aspects, *Biochem. Eng. J.*, 38(1), 2008, 61-69.
- [24]. W.J. Weber, and J.C. Morris, Kinetics of adsorption on carbon from solution, *J. Sanit. Eng. Div. Am. Soc. Civ. Eng.* 89(1), 1963, 31-60.
- [25]. G.E. Boyd, A.W. Adamson, and L.S. Myers, The exchange adsorption of ions from aqueous solutions by organic zeolite ii: Kinetics, *Journal of American Chemical Society*, 69, 1947, 2836-2848.
- [26]. Z. Aksu, Determination of the equilibrium, kinetics and thermodynamic parameters of the batch biosorption of lead (ii) ions onto *chlorella vulgaris*, *Process Biochem.*, 38, 2002, 89-99.
- [27]. R. Han, Z. Lu, W. Zou, W. Daotong, J. Shi, and Y. Jiujun, Removal of copper (ii) and lead (ii) from aqueous solution by manganese oxide coated sand: Equilibrium study and competitive adsorption, *Journal of Hazardous Materials*, 137, 2006, 480-488.
- [28]. F. Xiao, and H.H. Ju-Chang, Comparison of biosorbents with organic sorbents for removing Copper (II) from aqueous solutions, *J. Environ. Man.*, 90, 2009, 3105-3109.
- [29]. N.A.A. Siti, H.S.I. Mohd, L.K. Md, and I. Shamsul, Adsorption process of heavy metals by low-cost adsorbent: A review, *World Applied Science Journal* 28(11), 2013, 1518-1530.
- [30]. I.E. Agbozu, and F.O. Emoruwa, Batch adsorption of heavy metals (Cu, Pb, Fe, Cr and Cd) from aqueous solutions using coconut husk, *African Journal of Environmental Science and Technology*, 8(4), 2014, 239-246.
- [31]. A.O. Eruola, The Kinetics and effects of pH on removal of Manganese, Cadmium and Lead from aqueous solution by maize cobs, *Global Journal of Science Frontier Research Chemistry*, 12(6), 2012, 28-38.
- [32]. K.K. Pandey, G. Prasad, and V.N. Singh, Use of wollastonite for the treatment of Cu (II) rich effluent, *Water, air and soil pollution*, 27, 1986, 287-296.
- [33]. M. Ajmal, R.A.K. Rao, J.A. Anwar, and R. Ahmad, Adsorption studies on rice husk: removal and recovery of Cd(II) from wastewater, *Bioresources Technology*, 86, 2003, 147-149.
- [34]. J. Lakatos, S.D. Brown, and C.E. Snape, Coals as sorbent for the removal and reduction of hexavalent chromium from aqueous waste streams, *Fuels*, 81, 2002, 691-698.
- [35]. M.A. Mohamed, S.A. Wanees, A.M.M Ahmed, and M.S. Adam, Adsorption studies on the removal of hexavalent chromium contaminated waste water using activated carbon and bentonite, *Chemistry Journal*, 2(3), 2012, 95-105.
- [36]. Y.S. Ho, Removal of Copper ions from aqueous solution by tree fern, *Water Resources*, 37, 2003, 2323-2330.

- [37]. V. Vadivelan, and K.V. Kumar, Equilibrium, Kinetics, Mechanism and Process design for the sorption of methylene blue onto rice husk, *Journal of Colloid and Interface Science*, 286, 2005, 90-100.
- [38]. D. Mohan, and K.P. Singh, Single and multi-component adsorption of cadmium and zinc using carbon derived from bagasse- an agricultural waste, *Water Research*, 36, 2002, 2304-2318.
- [39]. R.P. Han, J.H. Zhang, W.H. Zou, J. Shi, and H.M. Liu, Equilibrium biosorption isotherm for Lead ion on Chaff, *J. Hazard Mater.*, B125, 2005, 266-271.
- [40]. R. Han, Z. Lu, W. Zou, W. Daotong, J. Shi, and Y. Jiujun, Removal of Copper (II) and Lead (II) from aqueous solution by Manganese oxide coated sand: Equilibrium study and competitive adsorption, *Journal of Hazardous materials* 137, 2006, 480-488.
- [41]. A.E. Elsayed, A.M. Mahdy, and N.H. Bbrakat, Thermodynamics of Copper desorption from soils as affected by citrate and succinate, *Soil and water Resources Journal*, 2(4), 2007, 135-140.
- [42]. M. Rounak-Shariff, and M. Kafia-Shareef, Thermodynamic adsorption of Herbicides on eight agricultural soils, *International Journal of Scientific and Engineering Research*, 2(6), 2011, 238-245.

(N. J. Okorocho). " Adsorption of Selected Heavy Metals Using Agricultural Waste: Equilibrium, Kinetic and Thermodynamic Studies" American Journal of Engineering Research (AJER), vol. 8, no. 12, 2019, pp 71-87